

RNA Labeling

International Edition: DOI: 10.1002/anie.201905949
German Edition: DOI: 10.1002/ange.201905949

Expanding APEX2 Substrates for Proximity-Dependent Labeling of Nucleic Acids and Proteins in Living Cells

Ying Zhou[†], Gang Wang[†], Pengchong Wang, Zeyao Li, Tieqiang Yue, Jianbin Wang, and Peng Zou^{*}

Abstract: The subcellular organization of biomolecules such as proteins and nucleic acids is intimately linked to their biological functions. APEX2, an engineered ascorbate peroxidase that enables proximity-dependent labeling of proteins in living cells, has emerged as a powerful tool for deciphering the molecular architecture of various subcellular structures. However, only phenolic compounds have thus far been employed as APEX2 substrates, and the resulting phenoxyl radicals preferentially react with electron-rich amino acid residues. This narrow scope of substrates could potentially limit the application of APEX2. In this study, we screened a panel of aromatic compounds and identified biotin-conjugated arylamines as novel probes with significantly higher reactivity towards nucleic acids. As a demonstration of the spatial specificity and depth of coverage in mammalian cells, we applied APEX2 labeling with biotin-aniline (Btn-An) in the mitochondrial matrix, capturing all 13 mitochondrial messenger RNAs and none of the cytoplasmic RNAs. APEX2-mediated Btn-An labeling of RNA is thus a promising method for mapping the subcellular transcriptome, which could shed light on its functions in cell physiology.

Eukaryotic cells feature highly compartmentalized cellular structures. In the past decade, a number of spatially restricted chemical labeling techniques have been developed to facili-

tate profiling of subcellular proteomes. These techniques often capitalize on genetically targetable enzymes that catalyze the formation of highly reactive intermediates, such as biotin-conjugated phenoxyl radicals^[1,2] or biotinyl 5'-adenylate^[3,4] in the cellular environment, which then react with neighboring biomolecules to achieve proximity-dependent labeling. Among these, enhanced ascorbate peroxidase APEX2 offers both high reactivity and high spatiotemporal resolution, and has been instrumental in revealing the proteomes of an array of subcellular compartments, including mitochondria,^[1,5-7] primary cilia,^[8] neuronal synapses,^[9] stress granules,^[10] and G-protein-coupled receptor signaling complexes.^[11,12] More recently, APEX2-mediated proximity labeling has been applied to map the subcellular transcriptome, either through crosslinking RNA to biotinylated proteins (APEX-RIP^[13] and Proximity-CLIP^[14]) or by directly biotinylating RNA (APEX-seq^[15]). All of the above studies have utilized the same APEX2 substrate: biotin-conjugated phenol (Btn-Ph). In the presence of hydrogen peroxide, APEX2 catalyzes the oxidation of Btn-Ph into a phenoxyl free radical, which reacts with electron-rich amino acid residues such as tyrosine in proteins.^[1,16,17]

In principle, the reactivity and lifetime of the APEX2-generated free radicals could be tuned through chemical modification of the aromatic ring. APEX2 has been reported to turn-over other aromatic substrates, but for purposes other than proximity-dependent labeling of biomolecules. These substrates include 3,3'-diaminobenzidine for creating electron microscopy contrast, guaiacol for colorimetric assays, and Amplex Red for fluorometric assays.^[18,19] This promiscuity in substrate recognition likely results from the wide binding pocket and the high oxidation power of ascorbate peroxidase, which upon activation by H₂O₂, forms Compound I with a redox potential as high as 1.16 V.^[20] We therefore sought to improve APEX2 labeling through expanding the scope of its substrates.

In this study, we screened a panel of aromatic APEX2 substrates for their reactivity towards proteins and nucleic acids. Among these, we discovered biotin-aniline (Btn-An) and biotin-naphthylamine (Btn-Nap) as novel probes with substantially higher reactivity towards RNA and DNA than Btn-Ph. Using mitochondrial matrix as an example, we demonstrated the power of subcellular transcriptome profiling with Btn-An, capturing all 13 mitochondrial messenger RNAs (MT-mRNA) and both ribosomal RNAs (MT-rRNA). We also demonstrated the high spatial specificity of APEX2-mediated Btn-An labeling in other subcellular compartments such as the nucleolus and the nucleoplasm. This expanded

[*] Y. Zhou,^[†] P. Wang, T. Yue, P. ZouCollege of Chemistry and Molecular Engineering, Synthetic and Functional Biomolecules Center, Beijing National Laboratory for Molecular Sciences, Key Laboratory of Bioorganic Chemistry and Molecular Engineering of Ministry of Education, Peking University Beijing, 100871 (China)
E-mail: zoupeng@pku.edu.cnG. Wang^[†]Academy for Advanced Interdisciplinary Studies
Peking University, Beijing, 100871 (China)G. Wang,^[†] P. Wang, Z. Li, J. Wang, P. Zou

Peking-Tsinghua Center for Life Sciences, Beijing, 100871 (China)

P. Wang, J. Wang

School of Life Sciences, Tsinghua University, Beijing, 100084 (China)

Z. Li

Peking-Tsinghua-NIBS Joint Graduate Program
Tsinghua University, Beijing, 100084 (China)

P. Zou

PKU-IDG/McGovern Institute for Brain Research
Beijing, 100871 (China)

[†] These authors contributed equally to this work.

Supporting information and the ORCID identification number(s) for the author(s) of this article can be found under:

<https://doi.org/10.1002/anie.201905949>

panel of APEX2 probes thus opens the door to novel DNA/RNA labeling applications.

We started by synthesizing seven biotin-conjugated aromatic substrates, including hydroxybenzamides, hydroxypicolinamides, aniline, and naphthylamine (Figure 1). These

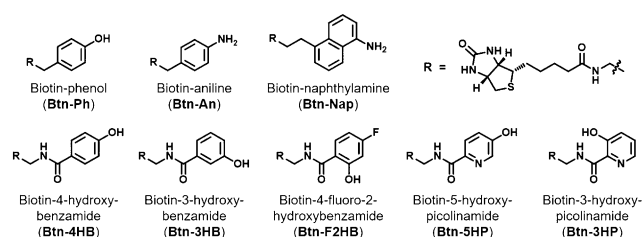


Figure 1. A panel of APEX2 substrates used in this study.

compounds differ in their redox potential and bond-dissociation energy.^[21–23] We evaluated their labeling reactivity towards proteins with purified APEX2,^[2] using bovine serum albumin (BSA) as a model protein. Western blotting revealed that hydroxybenzamides (Btn-3HB and Btn-4HB) and aniline (Btn-An) are more reactive than Btn-Ph (Figure S1 in the Supporting Information). However, when we tested these substrates on human embryonic kidney (HEK) 293T cell lysate, we observed the highest labeling intensity with Btn-Ph, followed by naphthylamine (Btn-Nap), Btn-An, and Btn-3HP (Figure 2A). The difference in the order of reactivity indicates that these probes may have different preferences for their protein targets. In the cellular environment, with mitochondrial matrix-targeted APEX2 in HEK293T cells, Btn-Ph also exhibited the highest labeling intensity, which is consistent with cell lysate labeling assay (Figure S2). We thus concluded that, over all, these new probes are inferior to Btn-Ph for proteomic applications.

We next turned to testing their reactivity on nucleic acids. While phenoxyl radicals have been shown to react with guanosine to form a covalent adduct,^[15,24–26] our dot-blot assay revealed weak Btn-Ph labeling signal on either DNA or RNA (Figure 2B,C). When testing the panel of new substrates, naphthylamine (Btn-Nap) emerged as the most reactive probe towards DNA, followed by Btn-4HB, Btn-An, and

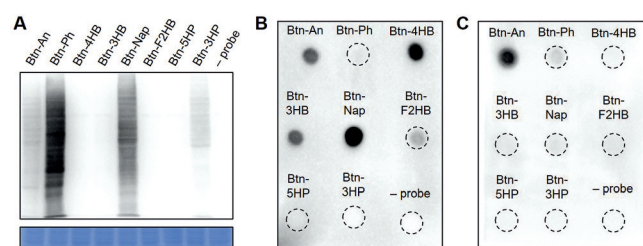


Figure 2. Comparison of APEX2 labeling activity of various probes on proteins, DNA, and RNA. A) APEX2-mediated protein labeling in whole-cell lysate extracted from HEK293T cells, followed by SDS-PAGE analysis. Top: Western blot. Bottom: Coomassie brilliant blue staining. B, C) Representative dot-blot images of APEX2-mediated labeling of plasmid DNA (B) and total RNA extracted from HEK293T cells (C). In all cases, biotinylation was initiated by mixing samples with purified APEX2 enzyme, biotin probes, and H₂O₂ in test tubes.

Btn-3HB (Figure 2B). Using synthetic oligonucleotides as substrates, we showed that Btn-Nap could label both double-stranded and single-stranded DNA (Figure S3). Interestingly, for RNA labeling, Btn-An yielded significantly higher signal than all other probes (Figure 2C), and was approximately 20-fold more efficient than Btn-Ph (Figure S4). Control experiments verified that biotinylation is dependent on both APEX2 and H₂O₂ (Figure S5). To further explore the capability of the aniline probe to label RNA, we synthesized five more biotin-conjugated aniline derivatives with various substitution groups on the aromatic ring, including -NO₂, -CF₃, -F, -CH₃, and -OH groups. Dot-blot analysis revealed that the simplest form of aniline, Btn-An, yielded the highest signal (Figure S6). Taken together, we have identified naphthylamine (Btn-Nap) and aniline (Btn-An) as novel APEX2 substrates with improved labeling efficiency towards nucleic acids. We focused on Btn-An for further investigation.

Because the sequences and structures of RNA vary considerably across the transcriptome, one might ask: to what extent do nucleobase composition and secondary structure of RNA influence its biotinylation efficiency? We employed synthetic oligonucleotides that lack one of the four nucleobases in their sequences, and compared their labeling intensities. Biotinylation signal was greatly reduced when guanosine (G) was removed from the oligonucleotide sequence, whereas removing the other three nucleobases (A, T, C) did not significantly affect labeling (Figure S7). In terms of secondary structure, we determined that Btn-An labeling on single-stranded RNA and DNA were 3.5 ± 1.2 -fold and 1.8 ± 0.3 -fold stronger than labeling on double-stranded DNA, respectively (Figure S8). The reaction yield of Btn-An labeling was quite low. We estimated from dot-blot analysis that biotinylation occurred approximately once per 2800 nucleotides on average (Figure S9). Given the low yield, we failed to identify the products of Btn-An labeling on ribonucleosides with liquid chromatography mass spectrometry (LC-MS; Figure S10).

To further evaluate the spatial specificity and sensitivity of APEX2-mediated RNA labeling in the context of living cells, we generated a HEK293T cell line that stably expresses APEX2 in the mitochondrial matrix (mito-APEX2; Figure 3A). Immunofluorescence imaging of labeled cells revealed that biotinylated targets were localized in close proximity to APEX2 (Figure 3B). Negative controls in the absence of the probe yielded negligible biotinylation signal (Figure S11). We extracted RNA from labeled cells and used streptavidin-coated beads to enrich biotinylated targets. The human mitochondrial genome encodes 37 genes comprising 13 MT-mRNAs, 2 MT-rRNAs, and 22 MT-tRNAs.^[27] Quantitative reverse transcription PCR (qRT-PCR) analysis showed clear enrichment of MT-mRNAs (from 12.3 ± 2.8 to 107.8 ± 31.6 fold) relative to the cytoplasmic mRNA marker *GAPDH* (Figure 3C). Treatment with RNase, but not DNase, reduced enrichment to background level, thus indicating that enriched samples were not contaminated with DNA (Figure S12). Compared with Btn-An labeling, the Btn-3HB and Btn-4HB probes failed to enrich mitochondrial mRNAs, while Btn-Ph labeling reduced enrichment levels by approximately 3-fold (Figure S13).

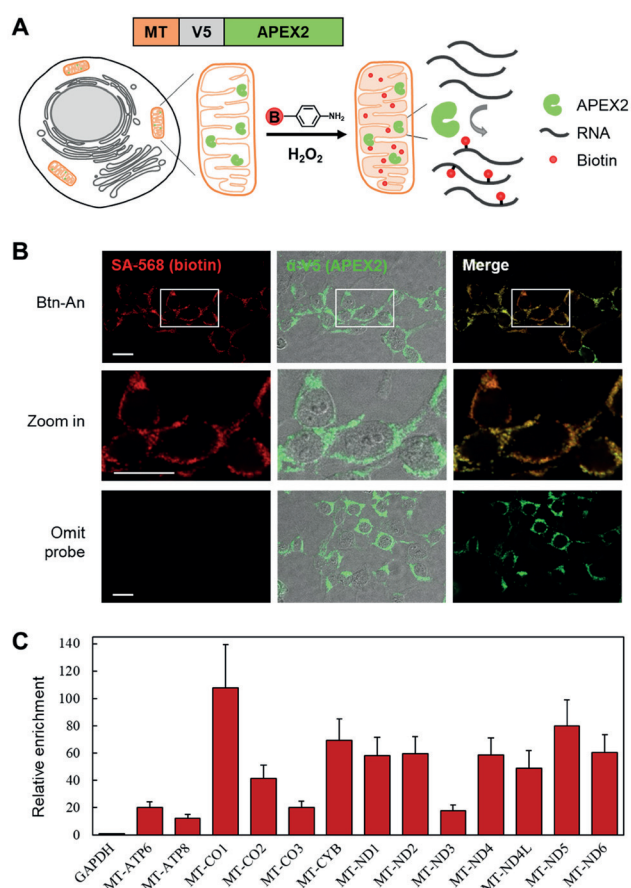


Figure 3. Fluorescence microscopy and qRT-PCR analysis of APEX2-mediated Btn-An labeling in HEK293T cells. A) Scheme of live-cell RNA labeling with Btn-An in the mitochondria. APEX2 was targeted to the mitochondrial matrix through fusion to the N-terminal 23 residues of the human COX4 (mito-APEX2). B) Immunofluorescence images of Btn-An labeling (left) and APEX2 expression (middle, overlaid with DIC images). Overlaid images of Btn-An and APEX2 are shown on the right. Top: HEK293T cells stably expressing mito-APEX2 labeled with Btn-An. Middle: Zoom-in of selected areas (white rectangle). Bottom: Negative control treated in the absence of Btn-An probe. Scale bars: 20 μm . DIC = differential interference contrast. C) Levels of enrichment for mitochondrial mRNAs as calculated from qRT-PCR analysis in four replicates, with GAPDH as the negative control. Error bars represent standard deviations.

Since qRT-PCR analyzes only a few genes at a time, we sought to characterize our labeling method at the transcriptome level with high-throughput sequencing. As outlined in Figure 4A, following biotinylation, RNA extraction, and affinity purification, eluted RNAs were reverse-transcribed and subjected to library construction (see the Supporting Information for details). As a quality control, the size distributions of DNA libraries were evaluated by capillary electrophoresis (Figure S14) before Illumina sequencing. We verified that APEX2 expression, Btn-An incubation, peroxide incubation, and nucleic acid labeling did not affect RNA abundance at the transcriptome level (Figure S15).

To quantify the level of enrichment, we calculated the fragments per kilobase of exon per million fragments mapped (FPKM) values for each gene before and after affinity

purification. We also compared FPKM values in labeled versus unlabeled control samples to eliminate potential bias introduced during affinity purification. In both cases, we defined the enrichment score as $\log_2(\text{FPKM}_{\text{enriched}}/\text{FPKM}_{\text{background}})$, where the background is either the input or the sample with the probe omitted. In total, we detected and quantified 9444 genes in the enriched sample, and their enrichment scores are plotted in Figure 4B. Consistent with our qRT-PCR analysis (Figure 3C), all 13 MT-mRNAs appeared clearly enriched (red), whereas abundant cytoplasmic mRNAs such as *ACTB* and *GAPDH* were not enriched (black, Figure 4B).

To quantitatively evaluate the spatial specificity and depth of coverage of APEX2-mediated Btn-An labeling, we performed three independent biological replicate experiments with the mito-APEX2 cell line and subsequently analyzed this dataset with DESeq2 software. As shown in Figure 4C, a total of 19 genes were significantly enriched (p -value < 0.0001 and $\log_2(\text{fold change}) > 2$), including all 13 MT-mRNAs and both MT-rRNAs. The remaining 4 genes included 1 mitochondrial tRNA (*MT-TP*) and 3 pseudogenes encoded by the mitochondrial genome (*MTATP6P1*, *MTND2P28*, *MTCO1P12*), and were thus expected to be enriched. RNA sequencing reads mapped almost uniformly along the gene length (Figure 4D and Figure S16). Together, the above data from qRT-PCR and next-generation sequencing established that APEX2-mediated Btn-An labeling is proximity-dependent and has sufficient sensitivity to profile transcriptome in live cells.

The post- vs. pre-enrichment fold change of mitochondrial RNA in our dataset varies substantially, ranging from 5 to 360 (Figure 4C). We also noticed a positive correlation of their enrichment levels across replicate experiments (Figure S17), thus suggesting that certain RNAs were more likely to be captured than the others. We wondered what caused this variability in labeling and enrichment. We found no correlation between enrichment and RNA length ($R^2 = 0.00$, Figure S18). Notably, enrichment levels of mitochondrial RNAs modestly and negatively correlated with their abundance ($R^2 = 0.56$) and lifetime ($R^2 = 0.52$, Figure S18), thus indicating that our method does not bias against RNAs that are short-lived or lowly expressed.

We tried to identify Btn-An labeling site on the RNA through analyzing mutations and stops in sequencing reads. However, we observed only 10 mutations in the mitochondrial transcriptome from enriched samples and no preference for particular nucleotides at sequencing read ends (Tables S1 and S2). Our sequencing sample preparation requires partial RNase digestion to yield primers for second strand synthesis, where the 3'-end nucleotide information is lost (see Supplementary Methods). This is in contrast to established RNA structure-mapping methods, such as SHAPE,^[28,29] which employed ligation-based approach for resolving the 3'-end of cDNA. Future efforts would focus on identifying the Btn-An labeling site and using this information to improve target identification accuracy, as well as mapping RNA structure.

To test the spatial specificity of APEX2-mediated Btn-An labeling in other subcellular locations, we targeted APEX2 expression to the nucleolus (FBL-APEX2) and the nucleo-

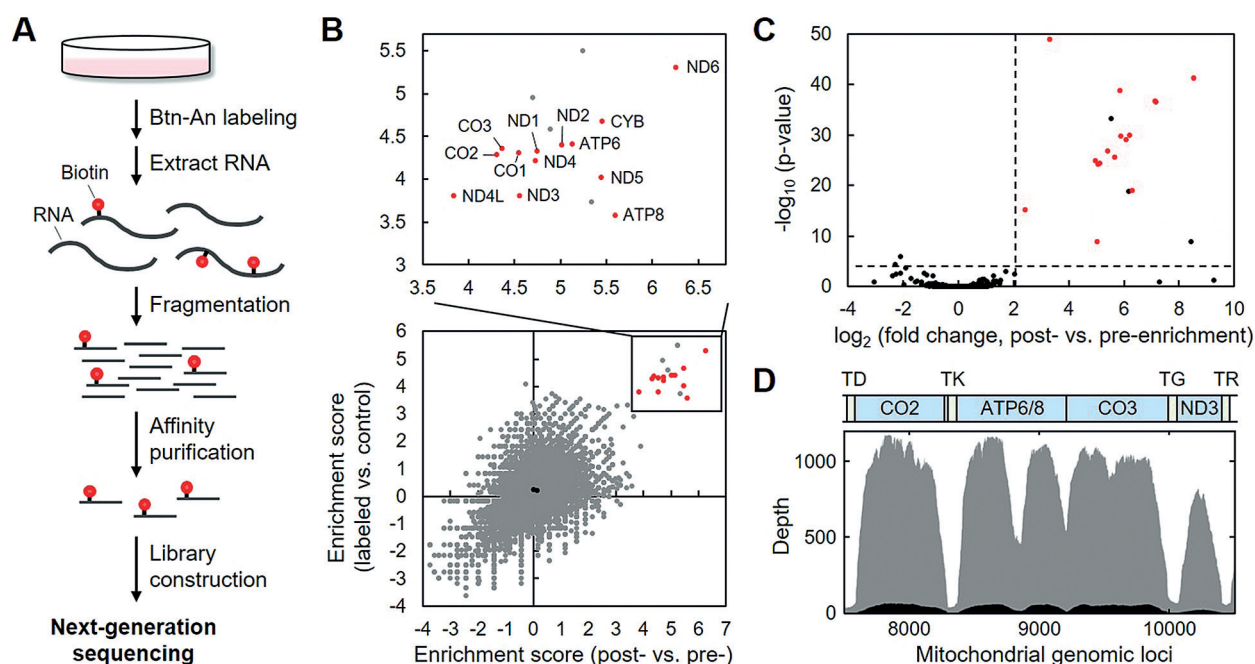


Figure 4. High-throughput sequencing analysis of mito-APEX2 labeling. A) Scheme of high-throughput sequencing workflow. B) Scatter plot of enrichment scores. Red dots represent 13 MT-mRNAs. Black dots are GAPDH and ACTB genes. Top panel shows zoom-in of the boxed region, with the names of mitochondrial mRNAs indicated. C) Transcriptome-wide analysis of gene-level RNA enrichment across three replicate experiments. Horizontal dash line indicates p -value = 0.0001. Vertical dashed line indicates the cutoffs for \log_2 (fold change) = 2. Red dots are MT-mRNAs, MT-rRNAs, and MT-tRNAs. Three black dots in the shaded region are mitochondrial pseudogenes. D) Nucleotide-level RNA enrichment across three replicates. Reads from enriched sample (grey) and the input (black) are mapped to the human mitochondrial genome (top).

plasm (H2B-APEX2) through protein fusion (Figure S19). We chose mitochondrial mRNAs MT-ND1 and MT-CO1 as negative markers. In the nucleolus, Btn-An labeling enriched small nucleolar RNA (snoRNA) U13, as expected. Interestingly, another snoRNA, U3, was not enriched in our dataset. In the nucleoplasm, small nuclear RNAs (snRNAs) 7SK and U1 were enriched by Btn-An labeling, whereas U13 and GAPDH were not (Figure S19). Together, these data demonstrate that APEX2-mediated Btn-An labeling could be applied to investigate the local transcriptome in various subcellular regions.

In summary, we have presented an expanded panel of APEX2 substrates and identified biotin-aniline (Btin-An) as a novel probe for efficient labeling of RNA in the cellular environment. We have demonstrated the exceptional spatial specificity and high sensitivity of RNA labeling in the mitochondrial matrix, the nucleoplasm, and the nucleolus. Because mitochondria are enclosed by two lipid layers, the strong Btin-An labeling signal indicates that this probe can easily permeate through cell membranes.

Arylamine-derived free radicals have been reported to attack the C-8 of guanine nucleobase, resulting in DNA damage.^[30,31] However, they have never been employed as probes for the purpose of local transcriptome profiling. Recently, APEX2-mediated proteomic labeling was combined with formaldehyde-mediated (APEX-RIP^[13]) or photo-induced (Proximity-CLIP^[14]) protein-RNA crosslinking to locally profile subcellular transcriptome. While these techniques have been applied to capture RNAs in various

subcellular compartments, including the mitochondrial matrix, the nucleus, the endoplasmic reticulum (ER) membrane, and the cell-cell interface, they do not directly target nucleobases and require additional crosslinking steps after APEX2 labeling, thus leading to poorer spatial resolution.^[13] APEX-seq solved these problems by directly labeling RNA with Btin-Ph.^[15] Our data showed that Btin-An could significantly improve RNA labeling efficiency both in vitro and in vivo (Figure 1 C and Figure S13). In principle, crosslinking methods such as APEX-RIP should preferentially capture RNA molecules with more protein-interaction partners, whereas APEX2-mediated Btin-An labeling of RNA favors capturing RNAs with fewer bound proteins. Therefore, these techniques may complement each other.

Acknowledgements

We thank Y. Li for assistance with chemical synthesis, W. Tang, R. Li, Z. Zou for helpful discussions. APEX2 plasmids were kind gifts from Dr. Alice Y. Ting (Stanford University). This work was supported by the National Key R&D Program of China (Ministry of Science and Technology, Grant 2017YFA0503600, 2018YFA0507600), the National Natural Science Foundation of China (Grant 91753131), Beijing Natural Science Foundation (5182011), the Interdisciplinary Medicine Seed Fund of Peking University (Grant BMU2017MC006), and Li Ge-Zhao Ning Life Science Junior Research Fellowship. PZ was sponsored by the

National Thousand Young Talents Award. We thank the National Center for Protein Sciences at Peking University in Beijing, China, for assistance with Fragment Analyzer 12.

Conflict of interest

The authors declare no conflict of interest.

Keywords: APEX2 · next-generation sequencing · proximity labeling · RNA · transcriptome

How to cite: *Angew. Chem. Int. Ed.* **2019**, *58*, 11763–11767
Angew. Chem. **2019**, *131*, 11889–11893

- [1] H. W. Rhee, P. Zou, N. D. Udeshi, J. D. Martell, V. K. Mootha, S. A. Carr, A. Y. Ting, *Science* **2013**, *339*, 1328–1331.
- [2] S. S. Lam, J. D. Martell, K. J. Kamer, T. J. Deerinck, M. H. Ellisman, V. K. Mootha, A. Y. Ting, *Nat. Methods* **2015**, *12*, 51–54.
- [3] K. J. Roux, D. I. Kim, M. Raida, B. Burke, *J. Cell Biol.* **2012**, *196*, 801–810.
- [4] T. C. Branon, J. A. Bosch, A. D. Sanchez, N. D. Udeshi, T. Svinkina, S. A. Carr, J. L. Feldman, N. Perrimon, A. Y. Ting, *Nat. Biotechnol.* **2018**, *36*, 880–887.
- [5] V. Hung, P. Zou, H. W. Rhee, N. D. Udeshi, V. Cracan, T. Svinkina, S. A. Carr, V. K. Mootha, A. Y. Ting, *Mol. Cell* **2014**, *55*, 332–341.
- [6] V. Hung, S. S. Lam, N. D. Udeshi, T. Svinkina, G. Guzman, V. K. Mootha, S. A. Carr, A. Y. Ting, *eLife* **2017**, *6*, e24463.
- [7] S. Han, N. D. Udeshi, T. J. Deerinck, T. Svinkina, M. H. Ellisman, S. A. Carr, A. Y. Ting, *Cell Chem. Biol.* **2017**, *24*, 404–414.
- [8] D. U. Mick, R. B. Rodrigues, R. D. Leib, C. M. Adams, A. S. Chien, S. P. Gygi, M. V. Nachury, *Dev. Cell* **2015**, *35*, 497–512.
- [9] K. H. Loh, P. S. Stawski, A. S. Draycott, N. D. Udeshi, E. K. Lehrman, D. K. Wilton, T. Svinkina, T. J. Deerinck, M. H. Ellisman, B. Stevens, S. A. Carr, A. Y. Ting, *Cell* **2016**, *166*, 1295–1307.
- [10] S. Markmiller, S. Soltanieh, K. L. Server, R. Mak, W. Jin, M. Y. Fang, E. C. Luo, F. Krach, D. Yang, A. Sen, A. Fulzele, J. M. Wozniak, D. J. Gonzalez, M. W. Kankel, F. B. Gao, E. J. Bennett, E. Lecuyer, G. W. Yeo, *Cell* **2018**, *172*, 590–604.
- [11] B. T. Lobingier, R. Huttenhain, K. Eichel, K. B. Miller, A. Y. Ting, M. von Zastrow, N. J. Krogan, *Cell* **2017**, *169*, 350–360.
- [12] J. Paek, M. Kalocsay, D. P. Staus, L. Wingler, R. Pascolutti, J. A. Paulo, S. P. Gygi, A. C. Kruse, *Cell* **2017**, *169*, 338–349.
- [13] P. Kaewsapsak, D. M. Shechner, W. Mallard, J. L. Rinn, A. Y. Ting, *eLife* **2017**, *6*, e29224.
- [14] D. Benhalevy, D. G. Anastasakis, M. Hafner, *Nat. Methods* **2018**, *15*, 1074–1082.
- [15] F. M. Fazal, S. Han, K. R. Parker, P. Kaewsapsak, J. Xu, A. N. Boettiger, H. Y. Chang, A. Y. Ting, *Cell* **2019**, *178*, 1–18.
- [16] N. D. Udeshi, K. Pedram, T. Svinkina, S. Fereshetian, S. A. Myers, O. Aygun, K. Krug, K. Clauser, D. Ryan, T. Ast, V. K. Mootha, A. Y. Ting, S. A. Carr, *Nat. Methods* **2017**, *14*, 1167–1170.
- [17] V. Hung, N. D. Udeshi, S. S. Lam, K. H. Loh, K. J. Cox, K. Pedram, S. A. Carr, A. Y. Ting, *Nat. Protoc.* **2016**, *11*, 456–475.
- [18] J. D. Martell, T. J. Deerinck, Y. Sancak, T. L. Poulos, V. K. Mootha, G. E. Sosinsky, M. H. Ellisman, A. Y. Ting, *Nat. Biotechnol.* **2012**, *30*, 1143–1148.
- [19] J. D. Martell, M. Yamagata, T. J. Deerinck, S. Phan, C. G. Kwa, M. H. Ellisman, J. R. Sanes, A. Y. Ting, *Nat. Biotechnol.* **2016**, *34*, 774–780.
- [20] I. Efimov, N. D. Papadopoulou, K. J. McLean, S. K. Badyal, I. K. Macdonald, A. W. Munro, P. C. Moody, E. L. Raven, *Biochemistry* **2007**, *46*, 8017–8023.
- [21] F. G. Bordwell, J. P. Cheng, *J. Am. Chem. Soc.* **1991**, *113*, 1736–1743.
- [22] F. G. Bordwell, X. M. Zhang, J. P. Cheng, *J. Org. Chem.* **1993**, *58*, 6410–6416.
- [23] K. U. Ingold, J. S. Wright, *J. Chem. Educ.* **2000**, *77*, 1062–1064.
- [24] J. Dai, M. W. Wright, R. A. Manderville, *Chem. Res. Toxicol.* **2003**, *16*, 817–821.
- [25] R. A. Manderville, *Can. J. Chem.* **2005**, *83*, 1261–1267.
- [26] J. Dai, A. L. Sloat, M. W. Wright, R. A. Manderville, *Chem. Res. Toxicol.* **2005**, *18*, 771–779.
- [27] T. R. Mercer, S. Neph, M. E. Dinger, J. Crawford, M. A. Smith, A. M. Shearwood, E. Haugen, C. P. Bracken, O. Rackham, J. A. Stamatoyannopoulos, A. Filipovska, J. S. Mattick, *Cell* **2011**, *146*, 645–658.
- [28] R. C. Spitale, P. Crisalli, R. A. Flynn, E. A. Torre, E. T. Kool, H. Y. Chang, *Nat. Chem. Biol.* **2013**, *9*, 18–20.
- [29] R. C. Spitale, R. A. Flynn, Q. C. Zhang, P. Crisalli, B. Lee, J. W. Jung, H. Y. Kuchelmeister, P. J. Batista, E. A. Torre, E. T. Kool, H. Y. Chang, *Nature* **2015**, *519*, 486–490.
- [30] R. Shapiro, S. Ellis, B. E. Hingerty, S. Broyde, *Chem. Res. Toxicol.* **1998**, *11*, 335–341.
- [31] M. Sproviero, A. M. Verwey, K. M. Rankin, A. A. Witham, D. V. Soldatov, R. A. Manderville, M. I. Fekry, S. J. Sturla, P. Sharma, S. D. Wetmore, *Nucleic Acids Res.* **2014**, *42*, 13405–13421.

Manuscript received: May 14, 2019

Revised manuscript received: June 24, 2019

Accepted manuscript online: June 26, 2019

Version of record online: July 26, 2019